Procedia Manufacturing

Volume 5, 2016, Pages 90–105

44th Proceedings of the North American Manufacturing Research Institution of SME http://www.sme.org/namrc

Milling Force Modeling: A Comparison of Two Approaches

Mark A. Rubeo and Tony L. Schmitz
University of North Carolina at Charlotte, Charlotte, NC
mrubeo@uncc.edu, tony.schmitz@uncc.edu

Abstract
This paper evaluates the dependence of cutting force coefficients on milling process parameters including feed per tooth, spindle speed, and radial immersion. Two methods are described for determining the cutting force coefficients: 1) the average force, linear regression method; and 2) the instantaneous force, nonlinear optimization method. A series of test cuts were performed and the cutting force coefficients calculated using the two methods are compared. Milling stability experiments were then conducted to validate the calculated cutting force coefficients. It was found that feed per tooth, spindle speed, and radial immersion exhibit a nonlinear relationship with the cutting force coefficients.

Keywords: Milling, stability, chatter, force, model, coefficients, regression, optimization

1 Introduction

The modeling of machining processes has been an important research topic for over a century and is motivated by the requirements of both machine tool users and builders. The machine tool user aims to reliably predict key process outputs, such as cutting forces, which affect workpiece surface quality, geometrical accuracy, and process stability. From the builder's perspective, the cutting forces represent a critical design metric because they dictate the required spindle power and torque as well as the required rigidity of the machine tool's structural loop. In machining process simulation and optimization, cutting force modeling strongly affects the accuracy of the results.

Mechanistic cutting force models assert that the instantaneous cutting forces are proportional to the uncut chip area through one or more empirical coefficients (Ehmann, et al., 1997). Early work in mechanistic force modeling for milling operations was reported by Martellotti (Martellotti, 1941), Koenigsberger et al. (Koenigsberger & Sabberwal, 1961), and Sabberwal (Sabberwal & Koenigsberger, 1961). The literature highlights two mechanistic force models. The first relates instantaneous cutting forces and uncut chip areas to the specific (cutting) force coefficient, K_s, and resultant cutting force angle, β. This single specific force coefficient captures the effect of both cutting

 Selection and peer-review under responsibility of the Scientific Programme Committee of NAMRI/SME
© The Authors. Published by Elsevier B.V.

doi:10.1016/j.promfg.2016.08.010

(shearing) and ploughing (due to friction at the cutting edge) which occurs during chip formation. The ease of implementation and predictive capabilities provided by this model have resulted in its widespread application in industry and research. The second, published in later work by Budak et al. (Budak, et al., 1996), extends the mechanistic cutting force model to include separate empirical coefficients to capture the chip formation mechanics of both shearing and ploughing.

In (Schmitz & Smith, 2008) and (Altintas, 2012) a method for the identification of the empirical coefficients, commonly referred to as cutting force coefficients, is presented. The procedure applies a linear regression of measured, average cutting forces over a range of feed per tooth values, while holding other process parameters, such as cutting speed and cut geometry, constant. This method requires numerous cutting tests and provides results which are specific to the selected cutting tool geometry and workpiece material combination. The regression analysis assumes that the cutting forces are linearly dependent on feed per tooth and independent of other machining parameters, such as cutting speed and feed, cut geometry, and cut direction (i.e., up milling/down milling). Other methods, such as those presented in (Gonzalo, et al., 2010) and (Campatelli & Scippa, 2012), use nonlinear optimization methods to perform a least squares fit of simulated cutting forces to measured cutting forces. This approach requires force measurement from just a single cutting test and, again, results in cutting force coefficients which are specific to the selected machining parameters. As such, the cutting force coefficients may be considered to be a function of not only the cutting tool geometry and workpiece material, but also machining parameters. The nonlinear optimization method provides a tool for studying the effects of these machining parameters on dynamic cutting forces.

In this paper, a study is described where the cutting force coefficients of the mechanistic force model are determined using both linear regression and nonlinear optimization methods. The paper is organized as follows. First, the mechanistic force model is detailed and the two methods (i.e., linear regression and nonlinear optimization) of cutting force coefficient determination are described. Next, the experimental method, which includes the cutting force measurement and the stability testing setup, is detailed. Finally, the resultant cutting force coefficients are compared and the practicality of the nonlinear optimization method is demonstrated in the framework of a milling stability prediction via time domain simulation and experimental validation. This is followed by a discussion of the experiment results and their impact on finish milling operations at low radial immersion.

2 Mechanistic Force Model

The mechanistic force models are based on the assumptions that: 1) the instantaneous cutting force is proportional to the cross sectional area of the uncut chip through empirical cutting force coefficients; and 2) the instantaneous cutting forces are independent of other machining parameters. Although this assumption provides a reasonable degree of accuracy for milling stability prediction using stability lobe diagrams (Schmitz & Smith, 2008), it has been shown that cutting forces are dependent on cutting speed and feed (Campatelli & Scippa, 2012). The mechanistic force model used in this study includes instantaneous cutting forces in the tangential, F_t, normal, F_n, and axial, F_a, directions and six corresponding cutting force coefficients; see Equations (1)-(3):

$$F_t = k_{tc} b h + k_{te} b \tag{1}$$

$$F_n = k_{nc} b h + k_{ne} b \tag{2}$$

$$F_a = k_{ac} b h + k_{ae} b \tag{3}$$

where b is the chip width (i.e., axial depth of cut in milling) and h is the instantaneous chip thickness, which is based on the circular tooth path approximation; see Equation (4):

$$h = f_t \sin(\phi) \tag{4}$$

where f_t is the feed per tooth and ϕ is the cutter rotation angle. Each component of the instantaneous cutting force includes two cutting force coefficients. The coefficients k_{tc}, k_{nc}, and k_{ac} are correlated with cutting and the edge coefficients k_{te}, k_{ne}, and k_{ae} are correlated with ploughing. The edge coefficients affect the instantaneous cutting force proportionally through the chip width, but are independent of the instantaneous chip thickness.

2.1 Average Force, Linear Regression Method

The six cutting force coefficients may be determined through linear regression analysis (Schmitz & Smith, 2008) using the average cutting forces measured during a series of cutting tests which were performed over a range of feed per tooth values while holding other milling parameters constant. Projecting the tangential, normal, and axial cutting force components into a fixed reference frame (i.e., x, y, and z), shown in Figure 1, and averaging over one cutter revolution yields the following expressions for mean cutting force per revolution.

$$\bar{F}_x = \left\{\frac{N_t b f_t}{8\pi}\left[-k_{tc}\cos(2\phi) + k_{nc}(2\phi - \sin(2\phi))\right] + \frac{N_t b}{2\pi}\left[k_{te}\sin(\phi) - k_{ne}\cos(\phi)\right]\right\}_{\phi_s}^{\phi_e} \tag{5}$$

$$\bar{F}_y = \left\{\frac{N_t b f_t}{8\pi}\left[k_{tc}(2\phi - \sin(2\phi)) + k_{nc}\cos(2\phi)\right] - \frac{N_t b}{2\pi}\left[k_{te}\cos(\phi) + k_{ne}\sin(\phi)\right]\right\}_{\phi_s}^{\phi_e} \tag{6}$$

$$\bar{F}_z = \left\{\frac{N_t b}{2\pi}\left[k_{ac} f_t \cos(\phi) - k_{ae}\phi\right]\right\}_{\phi_s}^{\phi_e} \tag{7}$$

where N_t is the number of teeth on the cutter and ϕ_s and ϕ_e are the start and exit angles of each tooth based on the radial depth of cut and cut direction. These expressions can be expanded and arranged in slope-intercept form.

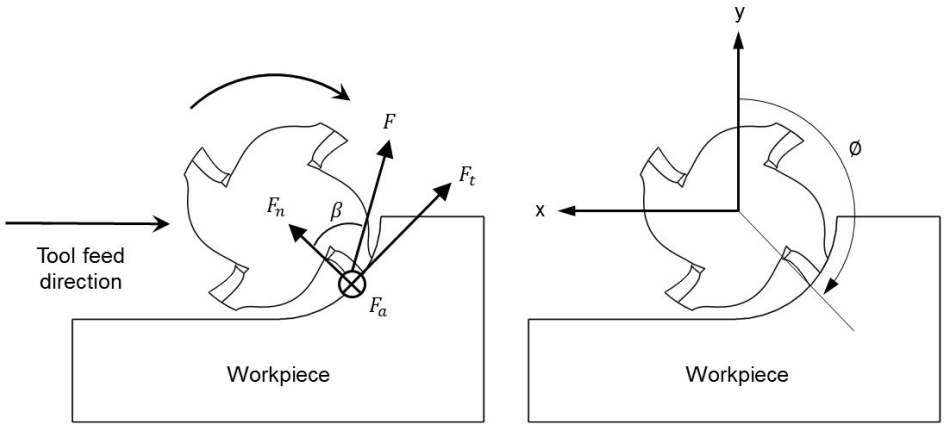

Figure 1. Force components and fixed reference frame for the average force, linear regression method. A down milling configuration is shown with a helical endmill.

Then, a linear regression over feed per tooth may be performed to determine the cutting force coefficients. The slope, a_{1j}, and intercept, a_{0j}, of the linear regression are given as:

$$a_{1j} = \frac{n\sum_{i=1}^{n} f_{t,i}\bar{F}_{j,i} - \sum_{i=1}^{n} f_{t,i}\sum_{i=1}^{n}\bar{F}_{j,i}}{n\sum_{i=1}^{n} f_{t,i}^2 - \left(\sum_{i=1}^{n} f_{t,i}\right)^2} \tag{8}$$

$$a_{0j} = \frac{1}{n}\sum_{i=1}^{n}\bar{F}_{j,i} - a_{1j}\frac{1}{n}\sum_{i=1}^{n} f_{t,i} \tag{9}$$

where j indicates the force component direction (i.e., x, y, or z) and n is the number of data pairs $(f_{t,i}, \bar{F}_{j,i})$. Once the slopes and intercepts are determined, the cutting coefficients may be calculated.

2.2 Instantaneous Force, Nonlinear Optimization Method

Alternatively, the cutting force coefficients may be identified using an instantaneous force, nonlinear optimization method which solves a nonlinear, least squares curve fitting problem and takes into account the user-defined lower and upper bounds on the decision variables (i.e., cutting force coefficients and flute-to-flute runout). The optimization routine, which uses a trust-region-reflective least squares algorithm, equates cutting forces simulated in the time domain with measured cutting forces at each discrete time step.

The time domain simulation calculates the cutting forces at each small time step, dt, which is defined in the simulation as:

$$dt = \frac{1}{f_s} \tag{10}$$

where f_s is the sampling frequency of the cutting force measurement. At each time step the instantaneous chip thickness is computed, the cutting force is calculated, the tooth angle, ϕ, is incremented by a small angle, $d\phi$, which depends on the spindle speed and the time step, and the process is repeated for one complete revolution of the cutting tool. The instantaneous chip thickness is determined using the circular tooth path approximation and assuming a rigid tool and workpiece

(although this is not strictly required). Additionally, flute-to-flute runout of the cutting tool is incorporated into the instantaneous chip thickness calculation.

The tangential, F_t, normal, F_n, and axial, F_a, cutting force components are calculated according to the mechanistic force model defined in the previous section. In order to represent the simulated forces in the fixed reference frame of the measured cutting forces, a coordinate transformation is performed:

$$\begin{Bmatrix} F_x \\ F_y \\ F_z \end{Bmatrix}_{simulated} = \begin{bmatrix} \cos(\phi) & \sin(\phi) & 0 \\ \sin(\phi) & -\cos(\phi) & 0 \\ 0 & 0 & 1 \end{bmatrix} \begin{Bmatrix} F_t \\ F_n \\ F_a \end{Bmatrix}_{simulated} \tag{11}$$

where ϕ is the instantaneous cutter rotation angle. The objective function is defined as:

$$f_i(k) = \begin{Bmatrix} F_x \\ F_y \\ F_z \end{Bmatrix}_i^{simulated} - \begin{Bmatrix} F_x \\ F_y \\ F_z \end{Bmatrix}_i^{measured} \tag{12}$$

where k is the vector of decision variables, which includes the six cutting force coefficients and the flute-to-flute runout of the cutting tool and $f_i(k)$ is the difference between the x, y, and z components of the instantaneous simulated and measured cutting forces at the ith time step.

Because the time step between each simulated instantaneous cutting force must coincide with the measured cutting forces, the size of the resulting system of equations depends on the sampling frequency of the measurement and the number of cutting tool revolutions (i.e., number of time steps) included in the optimization. The nonlinear, least squares curve fitting problem takes the form:

$$\min_k \|f(k)\|_2^2 = \min_k (f_1(k)^2 + f_2(k)^2 + \cdots + f_n(k)^2) \tag{13}$$

where n is the number of time steps. The curve fitting problem is solved via a trust-region-reflective algorithm, which is based on an interior-reflective Newton approach that is well suited for solving nonlinear optimization problems where the decision variables are bounded by upper and/or lower limits (Coleman & Li, 1994).

For this study, the measured cutting forces were partitioned into 100 individual revolutions of the cutting tool and averaged; see Figure 2. The measured cutting forces exhibited a high degree of repeatability from one revolution of the cutting tool to the next. The average measured cutting force components were then used for the nonlinear optimization function along with a number of relevant process parameters, including the number of teeth on the cutting tool, sampling frequency of the force measurement, and initial guesses for the decision variables (i.e., cutting force coefficients and flute-to-flute runout).

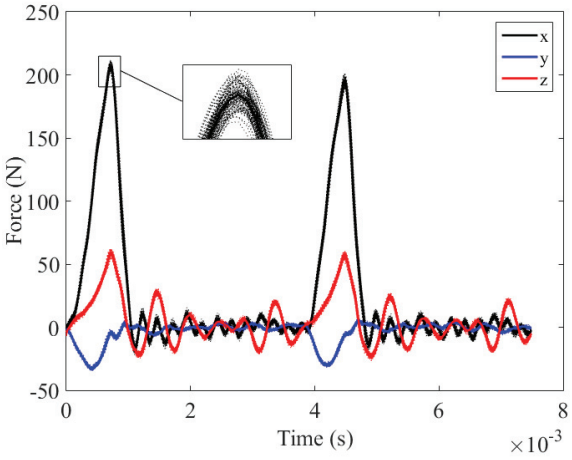

Figure 2. Measured cutting forces over 100 revolutions of the cutting tool (dotted line) and their average (solid line) shown for a milling operation using a two-flute cutting tool.

The optimization function simulates the instantaneous cutting forces in the x, y, and z directions based on the input process parameters. The difference between the simulated and measured cutting forces is then calculated by the objective function and the sum of squares of the differences is evaluated. The evaluation is then examined against an arbitrary, user-defined set of convergence criteria, such as the change in the sum of the squares from one iteration to the next. If it is determined that the convergence criteria are met, the optimization routine ceases; otherwise, the decision variables are updated and the process iterates until convergence. Example results of the optimized, simulated cutting forces are shown in Figure 3. Good agreement between the measured and simulated cutting forces is observed.

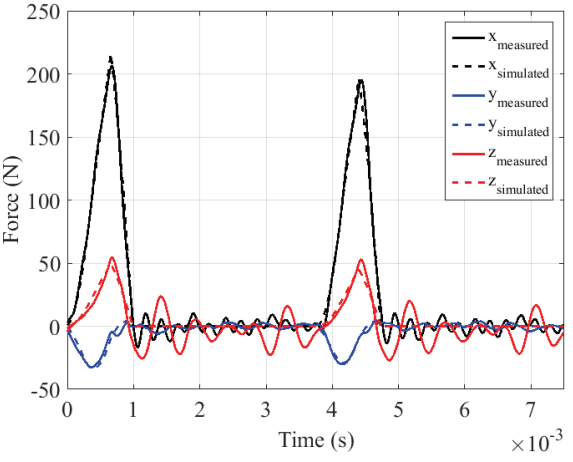

Figure 3. Example results from the nonlinear, optimization method including the measured cutting forces and optimized, simulated cutting forces.

3 Experiment Description

3.1 Cutting Force Measurement

Cutting tests were performed on a LeBlond Makino A55 Plus horizontal milling machine with a maximum spindle speed of 20000 rpm. The workpiece material was aluminum 6061-T6511 extruded barstock with approximate dimensions of 170 mm × 100 mm × 38 mm. It was rigidly fixed to the three-component cutting force dynamometer (Kistler 9257B) via two M8 socket head cap screws; see Figure 4. The dynamometer/workpiece combination was bolted to the machine tool's tombstone via a surface ground steel plate approximately 25 mm in thickness and was aligned to the machine axes using a test indicator. A charge amplifier (Kistler Type 5010), signal analyzer (Data Translation DT9837B), and data acquisition software (Spinscope, Manufacturing Laboratories, Inc.) were used to record the cutting force.

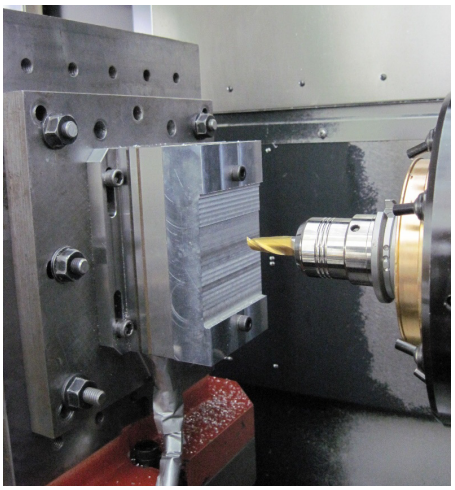

Figure 4. Setup for cutting force measurements using a three-axis dynamometer.

The cutting tool used in this study was a 12.7 mm diameter solid carbide endmill (SGS 39363) with a 30° helix angle. It was clamped in a Schunk SINO-R tool holder with approximately 40 mm of overhang. Cutting tests were performed with the tool in two conditions: 1) two flutes; and 2) single flute (i.e., one flute removed).

Cutting tests were performed under stable milling conditions with an axial depth of cut of 3 mm. Other process parameters, such as radial depth of cut, spindle speed, and feed per tooth (i.e., up/down milling), were varied. Details of the cutting force tests are listed in Table 1. Each cutting force measurement was repeated three times to enable a statistical analysis while minimizing the effect of tool wear on the measured cutting forces.

Table 1. Milling process parameters selected for cutting force measurements.

Cut direction	Radial immersion [%]	Spindle speed [$krpm$]	Feed [$mm/tooth$]
Up milling	10	8	(0.025, 0.05, 0.10, 0.15, 0.20, 0.25)

Down milling	10	8	$(0.025, 0.05, 0.10, 0.15, 0.20, 0.25)$
Down milling	10	$(1, 2, 3, 4, 6, 8, 10, 12.5, 15, 17.5, 20)$	0.10
Down milling	$(10, 30, 50)$	8	0.10

3.2 Validation Testing

The validity of the instantaneous force, nonlinear optimization method of calibrating the mechanistic force model is evaluated in the framework of milling stability experiments. The feed per tooth dependence of the cutting force coefficients was evaluated experimentally by performing a series of milling cuts on a system with fixed dynamics. The milling cuts were performed at the same axial depth of cut-spindle speed combinations while varying the feed per tooth. Stability predictions were performed using peak-to-peak (PTP) force diagrams, which are generated by multiple executions of a time domain simulation. The time domain simulation is based on the "Regenerative Force, Dynamic Deflection Model" described by Smith and Tlusty in (Smith & Tlusty, 1991). Additional details of the time domain simulation are given in (Schmitz & Smith, 2008) and the PTP force diagram is presented by Smith et al. in (Smith & Tlusty, 1993).

In order to facilitate the evaluation of stability in the validation tests, the system dynamics were controlled via a single degree-of-freedom, parallelogram type flexure, shown in Figure 5. The flexure provides a convenient method for evaluating the stability of the milling process by, ideally, constraining vibration to a single, flexible direction. Modal parameters for the combined flexure/workpiece system were obtained via impact testing using a modal hammer (PCB 086C04) to provide the excitation force and a low mass accelerometer (PCB 352C23) to record the response. Table 2 lists the natural frequency, f_n, modal stiffness, k, and dimensionless, viscous damping ratio, ζ, for the single degree-of-freedom flexure in the feed direction (i.e., x).

Table 2. Modal parameters for flexure in the $\boldsymbol{x}$ (feed) direction.

$f_n\ [Hz]$	$k\ [N/m]$	ζ
236.7	5.03×10^6	0.0097

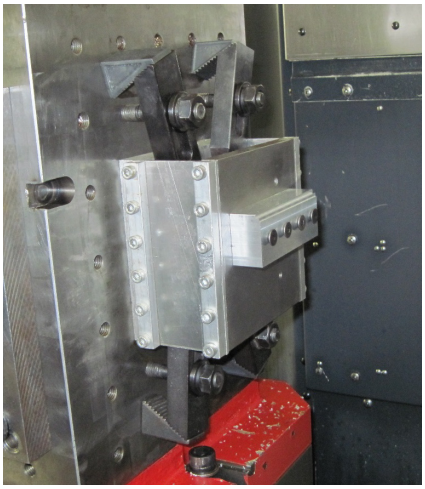

Figure 5. Setup for validation testing. The parallelogram type flexure and attached workpiece are mounted to the machine tool's tombstone.

The validation tests were performed using the same cutting tool previously detailed (SGS 39363). A low mass accelerometer (PCB 352C23) was used to measure the acceleration of the flexure/workpiece system during cutting. The frequency content of the acceleration signal was used to distinguish between stable and unstable milling conditions. Unstable milling operations were characterized by acceleration signals containing significant frequency content at or near the flexure's natural frequency, while stable milling conditions contained only frequency content at the tooth passing frequency and its harmonics.

4 Experiment Results

4.1 Feed per Tooth Dependence

The following experimental results compare the cutting force coefficients calculated using the average force, linear regression and instantaneous force, nonlinear optimization methods over a range of feed per tooth values. The cutting force measurements were repeated three times for each of the selected feed per tooth values, which are given in Table 1.

Figure 6 shows the result of the average force, linear regression analysis of the measured cutting forces over the range of feed per tooth values. A satisfactory fit was achieved as indicated by the coefficients of determination, r^2. The reported, measured cutting forces reflect the average forces calculated over the three repeated measurements. The calculated cutting force coefficients are provided in Table 3.

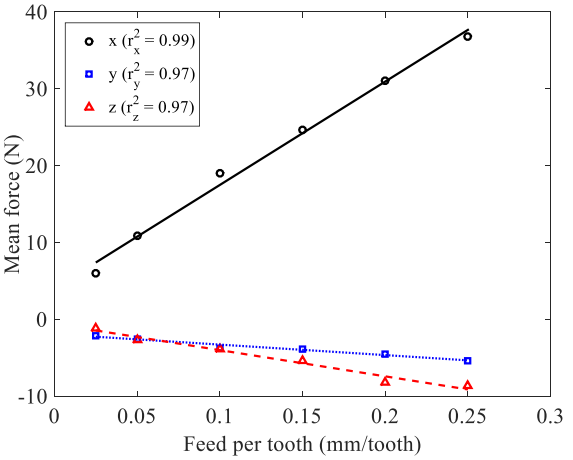

Figure 6. Average force, linear regression results from the 10% radial immersion up milling cut conducted at a spindle speed of 8000 rpm.

Table 3. Cutting force coefficients calculated using the average force, linear regression method for the 10% radial immersion up milling cut conducted at a spindle speed of 8000 rpm.

Cutting force coefficients $[N/mm^2]$		Edge force coefficients $[N/mm]$	
k_{tc}	805	k_{te}	6
k_{nc}	418	k_{ne}	6
k_{ac}	227	k_{ae}	1

The cutting force coefficients determined using the instantaneous force, nonlinear optimization method over the range of selected feed per tooth values are provided in Figure 7. The mean values of the three repeat measurements are reported along with the 95% confidence interval, which was calculated using the t-distribution. It is observed that the tangential and normal cutting force coefficients vary nonlinearly with feed per tooth as reported by other researchers (Campatelli & Scippa, 2012). No observable trend was noted in the edge force coefficients.

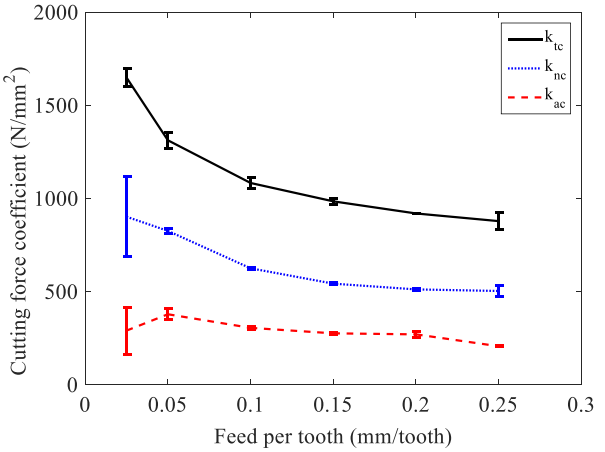

Figure 7. Cutting force coefficients calculated using the instantaneous force, nonlinear optimization method for a 10% radial immersion up milling cut conducted at a spindle speed of 8000 rpm.

The instantaneous, uncut chip thickness as seen by the cutting tool as each flute engages in the cut is influenced by both the commanded feed per tooth and percent radial immersion. For example, if the commanded feed per tooth is held fixed and percent radial immersion is decreased, the instantaneous, uncut chip thickness also decreases. To study the effects of radial immersion on the cutting force coefficients, a series of cutting tests were performed at 10%, 30%, and 50% radial immersion, while holding other milling parameters fixed. The resulting tangential cutting force coefficients, calculated using the instantaneous force, nonlinear optimization method, are reported in Figure 8 along with the 95% confidence intervals. A statistically significant variation in the tangential cutting force coefficient as a function of radial immersion may be observed. A similar trend in the normal direction coefficient was observed. However, an overlap of the 95% confidence interval precluded a statistically significant result.

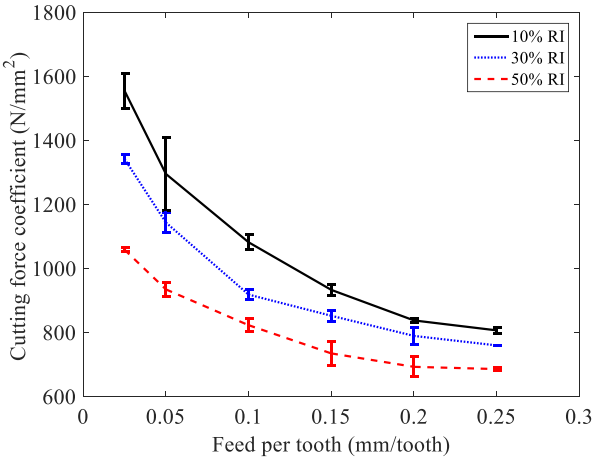

Figure 8. The tangential cutting force coefficient, calculated by the instantaneous force, nonlinear optimization method, as a function of radial immersion.

4.2 Cutting Speed Dependence

A series of cutting tests were performed over a range of spindle speeds and the force coefficients were calculated using the instantaneous force, nonlinear optimization method. The averaged results and 95% confidence intervals are displayed in Figure 9. The resulting trend is in good agreement with results published by Grossi et al. (Grossi, et al., 2014) (Grossi, et al., 2015). It is noteworthy that there is a general downward trend in the force coefficients until the critical spindle speed of approximately 12500 rpm. Beyond this critical spindle speed, there is a general upward trend. Typically the downward trend is attributed to thermal softening of the workpiece material due to the increased temperature at the tool/chip interface at high cutting speeds.

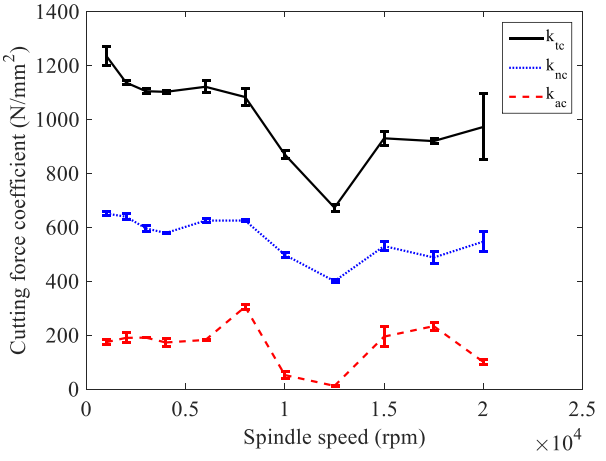

Figure 9. Cutting force coefficients calculated using the instantaneous force, nonlinear optimization method over the range of selected spindle speeds for the 10% radial immersion down milling operation.

4.3 Validation Testing

Validation testing was conducted at two feed per tooth values, $0.05\ mm/tooth$ and $0.25\ mm/tooth$, for a 10% radial immersion down milling cut. The cutting force coefficients were calculated using the instantaneous force, nonlinear optimization method. The results are provided in Figure 10 and Table 4. It was determined that the endmill exhibited approximately 30 μm of flute-to-flute runout. At low feed per tooth values (i.e., $0.025\,mm/tooth$) only one tooth was engaged in the cut per revolution and, as a result, the cutting force coefficients are higher at low feed per tooth values than reported for other cutting tools of similar geometry.

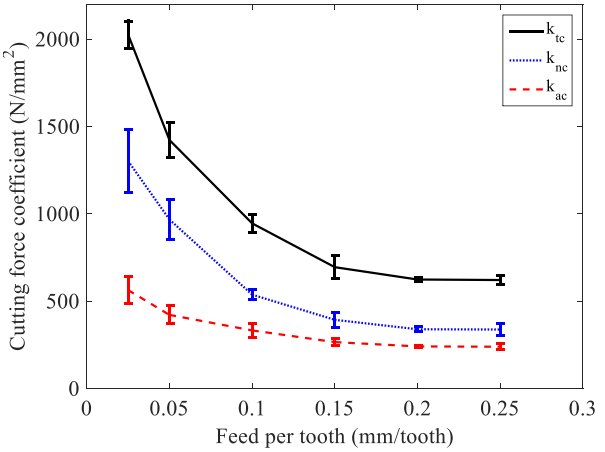

Figure 10. Cutting force coefficients calculated using the instantaneous force, nonlinear optimization method for a 10% radial immersion down milling cut conducted at a spindle speed of 8000 rpm.

Table 4. Cutting force coefficients used for milling stability predictions using the PTP force diagram.

Feed per tooth $[mm/tooth]$	Cutting force coefficients $[N/mm^2]$		Edge force coefficients $[N/mm]$	
0.05	k_{tc}	1422	k_{te}	16
	k_{nc}	967	k_{ne}	13
	k_{ac}	421	k_{ae}	0
Feed per tooth $[mm/tooth]$	Cutting force coefficients $[N/mm^2]$		Edge force coefficients $[N/mm]$	
0.25	k_{tc}	620	k_{te}	34
	k_{nc}	337	k_{ne}	20
	k_{ac}	239	k_{ae}	0

The PTP force diagram is conceptually similar to the traditional stability lobe diagram in the sense that it provides a map of stable and unstable axial depth of cut-spindle speed combinations. It conveys this information as a contour map of PTP cutting forces generated from numerous time domain simulations. The time domain simulation takes into account the tool and workpiece dynamics in three orthogonal directions as well as various parameters such as flute-to-flute runout and helix angle. The PTP force diagram generated using the cutting force coefficients for a feed rate of $0.05\ mm/tooth$ is shown in Figure 11. The results of the validation test cuts are included.

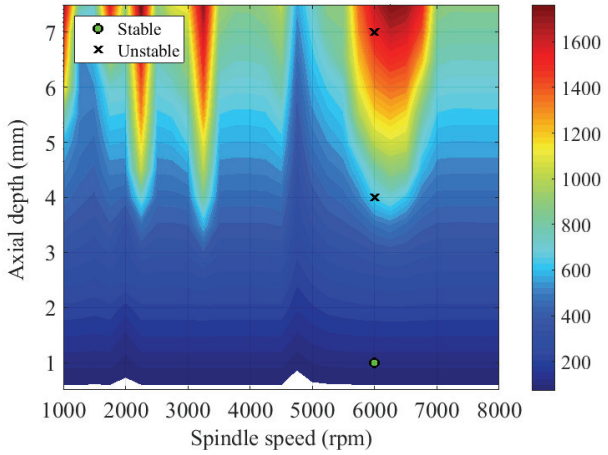

Figure 11. PTP force diagram generated using the cutting force coefficients calculated for a feed rate of $\mathbf{0.05\ mm/tooth}$. Stable (circle) and unstable (cross) validation test results are shown.

The resulting PTP force diagram generated using the cutting force coefficients for a feed rate of $0.25\ mm/tooth$ is shown in Figure 12. The results of the validation test cuts are included. It was observed that in both cases the PTP force diagram accurately predicted stable and unstable axial depth of cut-spindle speed combinations. Furthermore it is observed that the validation tests conducted at a 4 mm axial depth of cut yielded different results. The lower feed rate cut produced unstable results while the higher feed rate cut was stable.

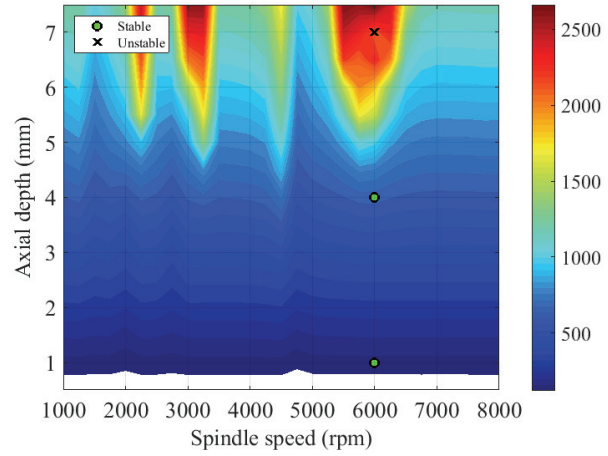

Figure 12. PTP force diagram generated using the cutting force coefficients calculated for a feed rate of $\mathbf{0.25\ mm/tooth}$. Stable (circle) and unstable (cross) validation test results are shown.

5 Conclusions

In this paper, a comparative study that examined the dependence of cutting force coefficients on milling process parameters, including feed per tooth, spindle speed, and radial immersion, was presented. The mechanistic force model was detailed and the methods for calibrating the model (i.e., determining the cutting force coefficients) were presented. Next, the cutting force coefficients, calculated using the average force, linear regression and instantaneous force, nonlinear optimization methods, for a range of milling process parameters were reported. Finally, the instantaneous force, nonlinear optimization method was validated in the framework of milling stability tests.

It was determined that low feed rates, which are often recommended for hard-to-machine materials, produce disproportionately larger cutting forces per uncut chip area than high feed rates, particularly for low radial immersion milling. From a practical standpoint, this becomes relevant for the finish milling of titanium preforms, which are often encountered in the aerospace industry. The results reported here suggest that high feed rates increase the critical axial depth of cut below which all spindle speeds yield stable milling operations.

With respect to chip formation, the rake angle (i.e., inclination of the cutting edge relative to the surface normal) depends on both the commanded feed per tooth and the radius of the milling tool's cutting edge radius. Although the cutting tool may have a positive rake angle at the macroscopic scale, as the commanded feed per tooth approaches the same order of magnitude as the cutting edge radius of the milling tool, shown in Figure 13, the effective rake angle becomes negative. This change in rake angle is accompanied by a change in the mechanism by which the chip is formed (Gunay, et al., 2004). Additionally, the negative rake angle serves to impose compressive stresses on the workpiece surface. These factors contribute to the increase in the cutting force coefficients at low values of feed per tooth. In Figure 13, where the cutting tool's rake face is to the right of the cutting edge, it is observed that although the cutting edge radius is on the order of approximately 30 μm, the length of the negative rake angle may be several times larger.

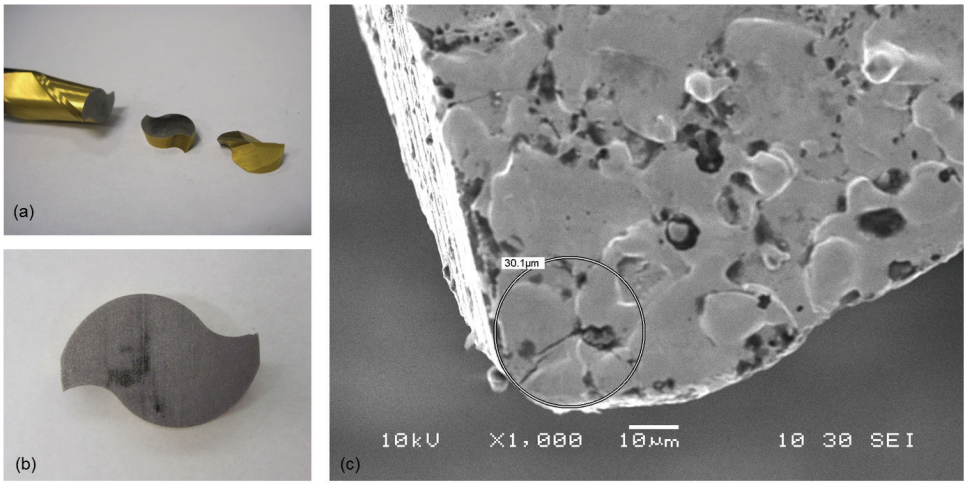

Figure 13. . A milling tool (a) cut into axial disks (b) to facilitate cutting edge radius measurements with a scanning electron microscope (c). In (c) the flank face is on the left and the rake race is on the right.

References

Altintas, Y., 2012. *Manufacturing automation: metal cutting mechanics, machine tool vibrations, and CNC design.* New York: Cambridge university press.

Armarego, E. & Brown, R. H., 1969. *The machining of metals.* Englewood Cliffs: Prentice-Hall Inc.

Budak, E., Altintas, Y. & Armarego, E., 1996. Prediction of milling force coefficients from orthogonal cutting data. *Journal of Manufacturing Science and Engineering,* pp. 216-224.

Campatelli, G. & Scippa, A., 2012. *Prediction of milling force coefficients for Aluminum 6082-T4.* s.l., s.n., pp. 563-568.

Coleman, T. F. & Li, Y., 1994. On the convergence of interior-reflective Newton methods for nonlinear minimization subject to bounds. *Mathematical Programming,* pp. 189-224.

Ehmann, K., Kapoor, S., DeVor, R. & Lazoglu, I., 1997. Machining process modeling: A review. *Journal of Manufacturing Science and Engineering,* pp. 655-663.

Feng, H.-Y. & Meng, C.-H., 1994. The prediction of cutting forces in the ball-end milling process-I. Model formulation and model building procedure. *International Journal of Machine Tools and Manufacture,* pp. 697-710.

Gonzalo, O., Beristain, J., Jauregi, H. & Sanz, C., 2010. A method for the identification of the specific force coefficients for mechanistic milling simulation. *International Journal for Machine Tools & Manufacture,* pp. 765-774.

Grossi, N., Sallese, L. & Campatelli, G., 2014. *Chatter stability prediction in milling using speed-varying cutting force coefficients.* s.l., s.n., pp. 170-175.

Grossi, N., Sallese, L., Scippa, A. & Camptatelli, G., 2015. Speed-varying cutting force coefficient identification in milling. *Precision Engineering,* pp. 321-334.

Gunay, M., Aslan, E., Korkut, I. & Seker, U., 2004. Investigation of the effect of rake angle on main cutting force. *International Journal of Machine Tools & Manufacture,* Volume 44, pp. 953-959.

Koenigsberger, F. & Sabberwal, A., 1961. An investigation into the cutting force pulsations during milling operations. *International Journal of Machine Tool Design and Research,* pp. 15-33.

Mackerle, J., 2003. Finite element analysis and simulation of machining: an addendum. A bibliography (1996-2002). *Journals of Machine Tools and Manufacture,* pp. 103-114.

Martellotti, M. E., 1941. An analysis of the milling process. *Transactions of the ASME,* pp. 677-700.

Merchant, M. E., 1944. Basic mechanics of the metal cutting process. *Journal of Applied Mechanics,* pp. 168-175.

Sabberwal, A. & Koenigsberger, F., 1961. Chip section and cutting force during the milling operation. *Annals of the CIRP,* p. 62.

Schmitz, T. L. et al., 2007. Runout effects in milling: Surface finish, surface location error, and stability. *International Journal of Machine Tools and Manufacture,* pp. 841-851.

Schmitz, T. L. & Smith, S. K., 2008. *Machining dynamics: frequency response to improved productivity.* New York: Springer Science & Business Media.

Smith, S. & Tlusty, J., 1991. An overview of modeling and simulation of the milling process. *Journl of Engineering for Industry,* pp. 169-175.

Smith, S. & Tlusty, J., 1993. Efficient simulation programs for chatter in milling. *CIRP Annals-Manufacturing Technology,* pp. 463-466.

van Luttervelt, C. et al., 1998. Present situation and future trends in modelling of machining operations progress report of the CIRP working group 'Modelling of Machining Operations'. *Annals of the CIRP,* pp. 587-626.